

One-dimensional Classical Gas in a Harmonic Trap with Repulsive Interaction

Zhiyu

Fudan University, Shanghai, China

I. INTRODUCTION

Controlled and tunable experimental realizations of confined quantum systems with ultracold atoms enable nonequilibrium studies of quantum many-body states in novel geometries. A common feature of many cold-atom experiments is the confinement of a many-body system in a harmonic trap. Trapping introduces many distinctive features which have no analog in uniform many-body states, including collective excitations such as breathing modes, dipole modes, and scissors modes. Such trap-related collective modes have been widely studied both experimentally and theoretically for continuum systems, especially in the mean-field regime, since the early days after quantum degeneracy was achieved with trapped atoms [1][2].

In mean-field perspective, the physics of atom gas in Bose-Einstein Condensation can be described by the Gross-Pitaevskii equation[3][4], where the breathing frequency for 1D Bose gas is calculated to be $\Omega_{GP} = \sqrt{3}\omega_0$. Meanwhile, the experiment of Ref.[5] has found a regime of interactions where the breathing-mode frequency approaches the Gross-Pitaevskii prediction. However, since mean-field approach which generally omit quantum fluctuation is successful in this problem, one may wonder how quantum effect plays the role in the breathing mode. Thus, a natural question would be asked is how breathing frequency is dependent on interaction for classical gas. Though generated in BEC, the breathing mode phenomenon is not restricted to BEC. For a classical gas, the breathing mode still can be excited with a quench. A good knowledge of classical version may help us understand the quantum question better. Surprisingly, to the best of our knowledge, all the literature focus on the breathing mode in BEC, without a careful study of their classical counterpart, which actually seems easier. Since this classical version question has not been answered yet, more study is needed.

One the other hand, in a non-equilibrium many-body system, a more intriguing question is about its thermalization or relaxation property. Thermalization is among the most fundamental process for a many-body interacting system. All systems do not thermalize. An example is the Fermi-Pasta-Ulam paradox [] which shows confinement in phase-space so that the system stay non-thermalized for a long time. A lot of research on thermalization property has been done in other classical system. Ref.[12][10] studied the one dimensional gravitational system with Lyapunov exponents. Ref.[6] studied the ring of harmonic oscillators and magnetic moment by examine the canonical distribution of a subsystem . In

our paper, we will also probe the system's thermalization time scales from the perspective of canonical distribution as well as Lyapunov exponent. With these approaches, we will show that the thermalization time scale manifest a competition between total energy and interaction energy, so there is not any singular behavior in the thermalization time scales except the trivial divergence at zero interaction.

This paper is organized as follows: In Section II, we perform a scaling to reduce the parameter of the system. In addition, we briefly observe the ground state and reveal two dynamically distinct regime of the system, i.e. strong interaction regime and weak interaction regime. In Section III, we evaluate the breathing frequency according to its mechanism, and compare that with our numerical simulation result. Besides, we also introduce a rotating frame method of treating this problem, which is a convenient tool to analyze simple harmonic systems. In section IV, we focus on the thermalization property. We first examine the canonical distribution of energy to find out the threshold of thermalization, i.e. under what parameter the thermalization time scale is very large. Then we point out that there are two kind of thermalization (or relaxation) behavior that could be measured in this system. In the end of this section, we measure the Lyapunov Exponent to quantify the time scales and confirm the former discussion.

II. PREPARATION

A. Scaling behaviour

We investigated the classical gas in harmonic trap with a repulsive interaction. We chose one of the simplest types of interaction:

$$F = \begin{cases} F = F_0 & , x < \sigma \\ F = 0 & , x > \sigma \end{cases} \quad (1)$$

so the Hamiltonian is

$$H = \frac{1}{2}m\omega_0^2 \sum_i x_i^2 + \frac{1}{2}m \sum_i v_i^2 + \sum_{|x_i - x_j| < \sigma} F_0 (\sigma - |x_i - x_j|) \quad (2)$$

It can be shown that Eq.2 can be rewrite into the following form:

$$\tilde{H} = \frac{1}{2} \sum_i \tilde{x}_i^2 + \frac{1}{2} \sum_i \left(\frac{d\tilde{x}}{d\tilde{t}} \right)^2 + \sum_{|\tilde{x}_i - \tilde{x}_j| < 1} F_0 (1 - |\tilde{x}_i - \tilde{x}_j|) \quad (3)$$

with the transformation:

$$\begin{cases} \tilde{H} &= \frac{H}{m\omega_0^2\sigma^2} \\ \tilde{x}_i &= \frac{x_i}{\sigma} \\ \tilde{t} &= \omega_0 t \\ \tilde{F}_0 &= \frac{F_0}{m\omega_0^2\sigma} \end{cases} \quad (4)$$

In this manner, we reduced number of the parameters in our model into three: \tilde{H} , \tilde{F}_0 , N . Equivalently, we set σ , ω_0 and m to 1 in our numerical simulation. Throughout, we will use “E” and “ F_0 ” to denote their reduced version \tilde{H} , \tilde{F}_0 .

B. Overview

1. Relation between Radius and Energy

The radius of the cloud R is defined as the root-mean-square of particles’ position $\{x_i\}$

$$R \equiv \left(\overline{x_i^2} \right)^{\frac{1}{2}} \quad (5)$$

. When E is very large, the interaction energy can be omitted, so E is dominated by the kinetic energy and potential energy of harmonic oscillators. Thus, $E = \omega_0^2 \sum_i x_i^2 = N\omega_0^2 R^2$

2. Ground states

For the ground state of this system, one could predict that

(1) When the σ is larger than the size of the cloud (in view of the scaling behavior, large σ is equivalent to small F_0 limit when we fix $\sigma = 1$), it can be easily shown that the ground state is crystal-like, since all every particle keeps an equal distance with its nearest neighbors, which is $\frac{2F_0}{\omega_0^2}$. The low-lying excitation is particles’ independent harmonic oscillation around their equilibrium position.

(2) When F_0 is very large the molecules act like a hardcore gas, while the size of particle is just σ .

In the fig.1, we can see this crossover from the “solid-like” limit (left) to the “hardcore gas” limit (right).

III. BREATHING FREQUENCY

Usually, to see the response of quantum gas to a quench, one begin simulation with the ground state and then suddenly vary some parameter by a little, for instance, $\omega'_0 \rightarrow \omega_0 = \omega'_0 + \Delta\omega$. In that case, one will observe the radius R oscillating at a certain frequency, which is usually called “breathing mode”. However, it

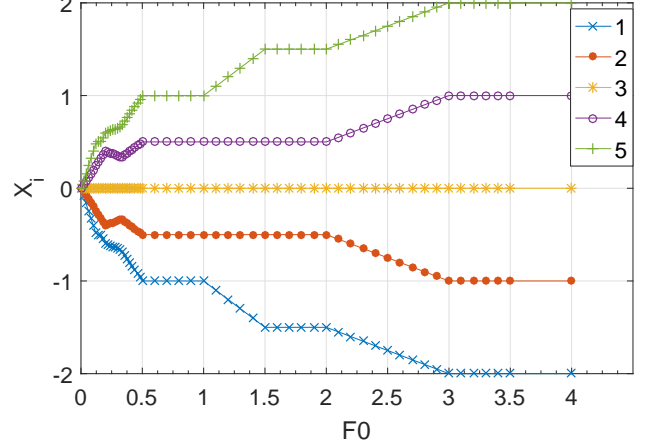


FIG. 1. particles’ position at ground states

is quite different in the classical version. Firstly, the ground state may be meaningless. In quantum case, the reason why we care about ground state and low lying excitations is that BEC occur at low temperature. But in classical case, there is no BEC. So it is not necessary to focus on low lying excitations in classical case. Besides, since classical limit is $\hbar \rightarrow 0$, no matter how low the kT is, \hbar/kT is always zero so that classical behaviour of low lying excitations is quite different from the quantum one. Secondly, it is no longer necessary to vary parameters “by a little” in the quench. In quantum case, the small quench $\omega'_0 \rightarrow \omega_0 = \omega'_0 + \Delta\omega$ means the spectrum is shifted slightly, thus one may expect to see some beat phenomenon(?). But in classical case, since \hbar vanishes, no matter how small the quench is, one can never recover or proximate the quantum case. Thus it is not necessary to limit ourselves to small quench.

Furthermore, notice that X and P (normalized) are symmetric for simple harmonic oscillator. In weak interaction limit, the distribution cloud should be circular when the gas is completely thermalized. The difference between thermalized cloud before and after quench is that they are circular under different normalization of phase-space. If we look at both of them in the phase-space normalized according to the final ω_0 , we will find shape of the cloud before the quench is an ellipse while the final one is a circle.

Since the number of particles we use in the Molecular Dynamics simulation is limited (usually 5 to 20), the random noise is significant. If we start with a state whose configuration in phase-space is an ellipse slightly deviated from circle, the oscillating amplitude will be too small to be distinguished from noise. Therefore, we start from an extreme case – line distribution (random x , zero p) and observe the oscillation of $R(t)$.

Without interaction, the breathing mode frequency is exactly 2. When there is interaction, the frequency will drift to some other value near 2. We measure the ra-

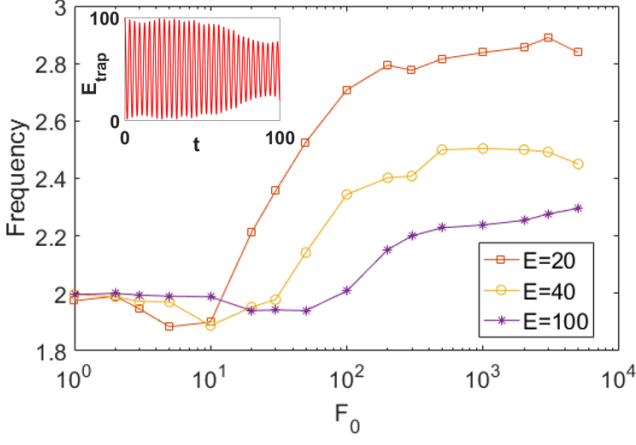


FIG. 2. breathing mode frequency measured at different E and F_0 . Insert: a demonstration of oscillation, E_{trap} is the total potential energy of particles in the trap, which is proportional to $\sum_{is} x_i^2$, thus manifest the oscillation behavior of radius $R(t)$ defined in Eq.5. The breathing frequency is measured by taking Fourier transformation of $R(t)$.

dius of the cloud $R(t)$ and get the frequency spectrum of its oscillation behavior by Fourier transform. Then we take the peak frequency near 2 as the breathing mode frequency. The frequency measured in different E and F_0 is shown in the Fig.2.

The mechanism that deviate breathing frequency from 2 is simple in real space. When two particle bounce, they exchange momentum immediately. It can be interpret as particle A carries its momentum P_A and jump σ to the right, while particle B carries its momentum P_B and jump σ to the left. In this manner, every collision will save a particle some time $\frac{\sigma}{v}$. Since v is proportional to R while the number of collision each particle experiences in one period of harmonic oscillation can be estimated by N , we will get $\delta \sim N^{\frac{3}{2}} E^{-\frac{1}{2}}$.

To see this picture better, let us first introduce a approach to simplify this problem:

A. Rotating frame in Phase-space

Traditionally, we think of there is a distribution cloud in phase space, and due to harmonic trap, the cloud will rotate at frequency ω_0 . When there is interaction, we may think there is a small modification of the frequency $\omega = \omega_0 + \delta$. Now we want to understand how δ is dependent on parameters, so it is better to stand in the rotating frame in the phase space. In this frame, the picture we will see is as follow:

- * All particles are stationary when there is no interaction.
- * The real X and P axis are rotating counter-clockwise, using real X axis to measure distance between particles

to determine the interaction at each moment.

- * When there is interaction, particles will gain a “velocity” in phase space: $\dot{P} = F/m$. Other effects are all cancelled by frame rotation.

This picture is actually a classical version of the interaction picture. With this picture, we will soon find the dynamic analysis greatly simplified.

In our system, we choose initial velocity to be zero, which means, the particles are aligned on $X|_{t=0}$ axis in phase-space at the beginning. If the breathing frequency of the system is $\omega = \omega_0 + \delta$, we will expect to see a line (which may gradually deform into an oval cloud or even an isotropic cloud) rotating at δ in rotating frame. If we plot x-p with t, we expect to see a spiral motion. Since the motion we see is an additional rotation in rotating frame, we will call it precession. This precession directly leads to the δ .

Fig.4 show this precession motion in the rotating frame in phase-space.

B. Estimating Breathing Frequency

Let us begin with two-particle case. When interaction is very strong, the effect of interaction is equivalent to exchanging momentum when two particles approach each other at distance σ . In the rotating frame in phase-space, this process can be interpret as follows:

(See fig.5(a)) Two particles flip to another line (thick gray line) which deviate a small angle α away from original configuration. Similar process happen when there are more particles. In every period of harmonic oscillation, each particle meet N particles and collide $2N$ times, while half of the collisions (N times) are between particles with huge difference in momentum, which is just the process shown in fig.5. (As for the remaining half of collisions, colliding particles have small difference in their momentum. Let us say, both particles have positive momentum. In fig.5, it can be shown that two particles on the same half of the P-axis cannot have strong effect on the rotation of distribution.)

Let us estimate the precession angle α in one collision by $\frac{\sigma}{R}$, which follows from the two-particle case study. Radius of the cloud R can be estimated according to $E = Nm\omega_0^2 R^2$ We will get the precession angular velocity

$$\delta = 2\omega_0 \frac{N^{\frac{3}{2}} m^{\frac{1}{2}} E^{-\frac{1}{2}} \sigma \omega_0}{2\pi} \quad (6)$$

When F_0 is not that large, the frequency behavior seems complicated (see fig.2). Usually, when F_0 increase, frequency goes down below 2 first and then rise up and converge to some value higher than 2. The reason could also be well understood with the mechanism described before. In the former discussion, we goes to high F_0 limit, which means particles exchange momentum in infinitesimal time. For F_0 is not very big, the finite interaction time should be taken into consideration. During

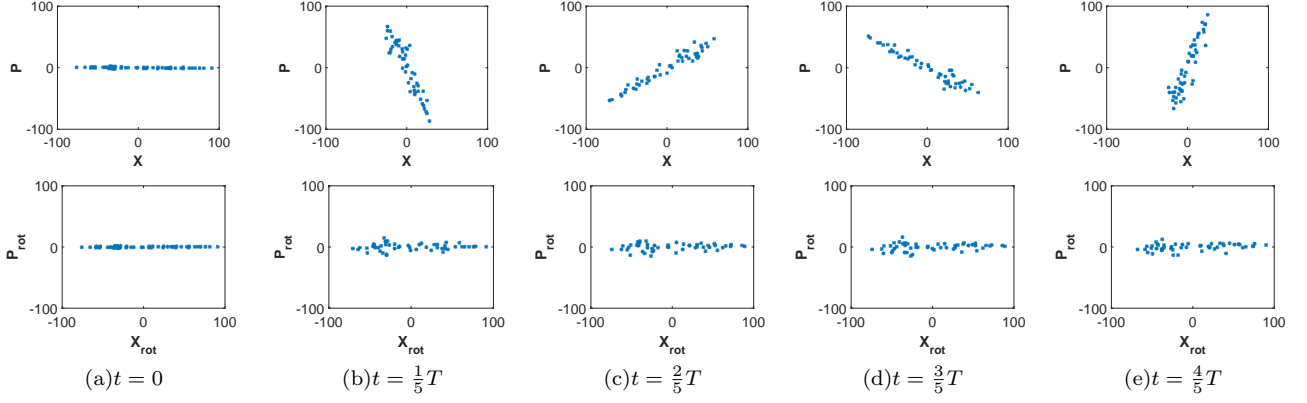


FIG. 3. $N=50, F_0=100, E=50000$. Upper(lower) five pictures are snapshot of the configuration of the cloud in the stationary(rotating) frame at $t=\frac{1}{5}T, \frac{2}{5}T, \frac{3}{5}T, \frac{4}{5}T, T$ respectively.

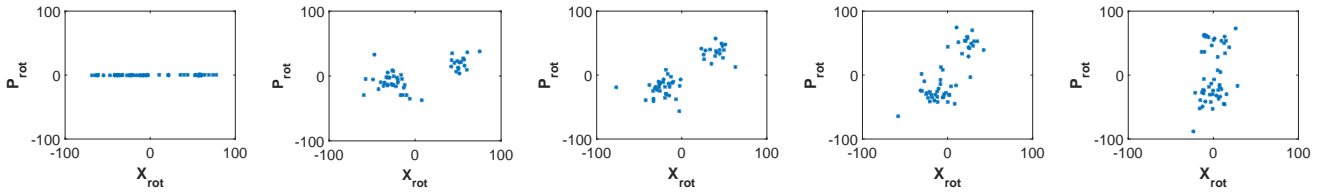


FIG. 4. the precession behavior of cloud viewed in the rotating frame in phase-space. $\frac{t}{T} = 0, 20, 40, 60, 80$

this time, the behavior of each particle in phase space is exactly moving along the direction of the real P axis at 'velocity' F_0/m . Since the real P axis is rotating counter-clockwise, the particle will follow the circular trajectory (orange and green dashed line in fig.5) the α that we once use to estimate the precession motion should decrease with the increase of interaction time. There should be some "critical point" where α goes from plus to minus (dashed green line). At this point, we will see the precession stop so that the frequency is 2.

The dependence of frequency on energy and F_0 is shown in fig.6. For the first thing, as expected when F_0 is high the frequency behavior is well-described by linear prediction Eq.6. Secondly, the figure shows the frequency's dependence on F_0 . As we explained, when F_0 is not so large, the precession angle decrease. In language of real space, the finite F_0 create a finite approaching time, thus consumes the time saved by finite-range collision. As a result, the frequency should be lower when F_0 decrease, and reach 2 earlier.

the critical point that frequency falls to 2 can be estimate by:

$$\omega_0 \tau = \alpha \quad (7)$$

which states that the approaching time τ exactly cancels the precession angle derived before τ can be estimated by R/F_0 . With some math, one can show that this condition is equivalent to

$$\frac{E}{N} = F_0 \sigma \quad (8)$$

which is the same as the criterion of whether two particle will bounce or pass by if one estimate the average internal energy of a pair with $\frac{E}{N}$. This argument indicate the reason why we see frequency stop falling down below 2 as one should expect with previous discussion: All our previous analysis based on fig.5 only studies the case of bouncing. If the energy of particles are so large that they often overcome the interaction potential barrier and pass each other, the situation would be completely different. In that case, in fig.5, particles will move a little bit out of their initial position, and soon move back, almost return to their initial place. In this manner, the interaction do not affect the distribution of the cloud in phase space. Thus, the frequency will stay near 2 when E is large.

Before completing the discussion, it is necessary to point out that none of the argument here require "energy thermalization". In addition, if the system is completely thermalized in terms of their phase of orbit in phase space, the argument will no longer work – there is a stable isotropic distribution in phase space, no matter how the cloud rotate, no oscillation can be observed.

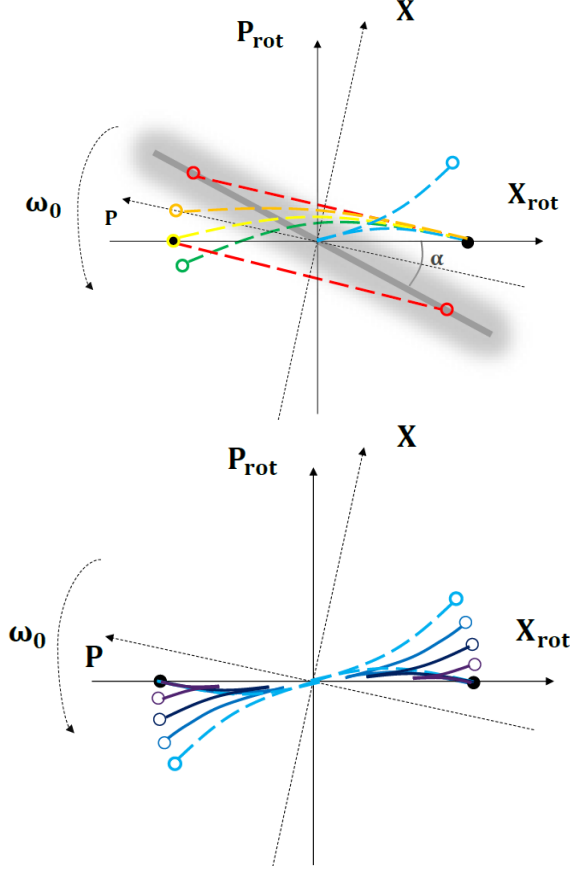


FIG. 5. a schematic diagram of the collision process: (a)(Upper)when $F_0 * \sigma$ is big, particles can not penetrate each other, thus their trajectory in rotating frame is a circular arc. (b) (Lower) When $F_0 * \sigma$ is small, particles easily pass each other, so that the force they feel is not continuous, their trajectory has a turning point(the dashed bright blue trajectory is identical with the one in the upper figure, which is the critical situation between passing and bouncing, that is to say, particles have zero relative velocity when they collide.)

IV. THERMALIZATION

A. Dynamics Study

It is natural to think that a many-body system with interaction will be thermalized in “usual” case. To study the condition of thermalization is equivalent to find out the mechanism that prohibits the system from ergodic. We begin the study with two-particle motion.

1. two particles

To see the way interaction change the orbit (energy level) of the particles, we had better start from two-particle case.

We can always think of them in the reference frame of their center of mass “C”. In frame C, one can easily

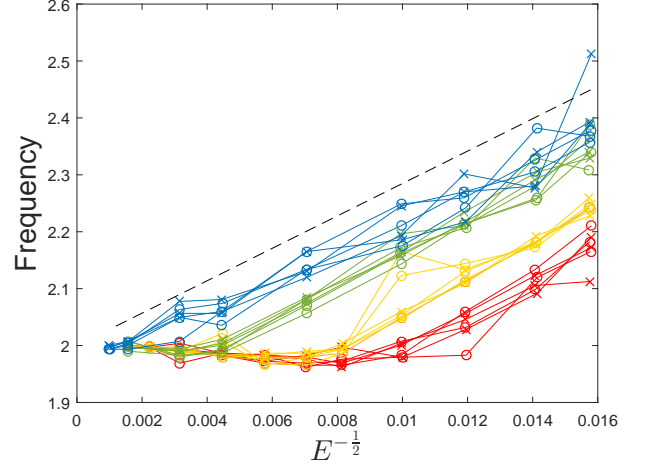


FIG. 6. dependence of breathing frequency on Energy, $N=20$. Different color stands for different F_0 : Red for $F_0=2000$; Yellow for $F_0=3000$; Green for $F_0=10000$; Blue for $F_0=100000$. Run with 3 different initial states in each case, and in each run, measure the frequency in 0-100 time unit(label as crosses) and in 900-1000 time unit (label as circles). The black dashed line is the prediction of Eq.6.

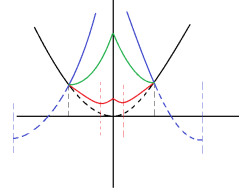


FIG. 7. effective potential for two-particle system

show that when there is no interaction what we will see is that two particles are bound together by a harmonic trap center at C (black line in fig.7). So their relative motion is also a harmonic oscillation.

In this case, the system has two frequency components. The first one is the frequency of C, which is just ω_0 . The other one is the frequency of their relative motion ω_r , which is slightly deviated from ω_0 . The deviation grows with the increase of F_0 and the decrease of internal energy of the pair. As a result, when the F_0 is small and when the E is large, a beat with low frequency $\omega_r - \omega_0 = \delta$ will exist. This phenomenon means energy transfer between particles are inefficient, thus it will slow down the thermalization process.

2. More particles

Now let's consider the three-particle case. For two particle, the motion is non-chaotic. On the other hand, intuitively, we will say that three-body motion is chaotic so

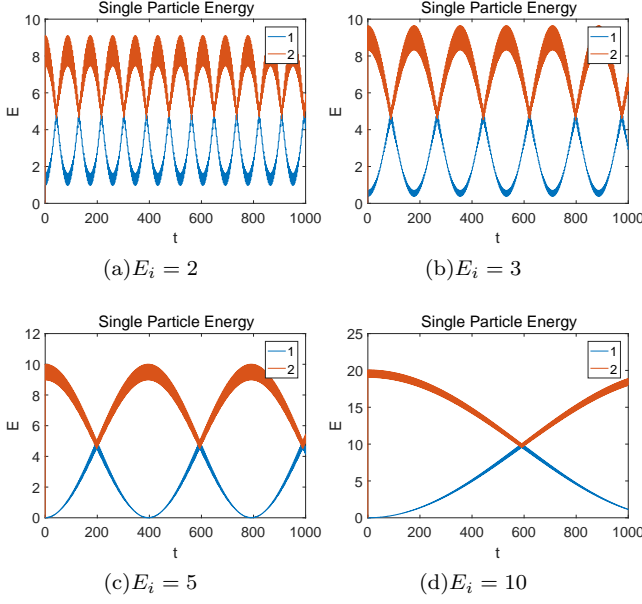


FIG. 8. the dependence of beat frequency on internal energy. The diagram is the energy of two particles. Here, F_0 is set to be 1. In this case, the larger E_i is, the lower the beat frequency is.

that the system could be “thermalized” soon. However, in some cases, the time scale of thermalizing could still be very long. Suppose two of them, say, A and B, has small internal energy, which means their distance and relative velocity are both small. Meanwhile, suppose particle C has some energy quite different from A & B. In this case, A & B will often be in the interaction, while C will pass both of them at a high speed in each period. How will energy transfer between C and the two-particle system A and B? Since the relative velocity of C and the two-particle system is usually large, C will pass A-B pair in a short time $\tau \sim \frac{\sigma}{R}$ ($\tau \ll \frac{2\pi}{\omega}$). C gives A a push when approaching it, and then push A back when leaving. As has been discussed in the two-particle case, this process is equivalent to giving A a very small velocity ($\sim O(\frac{\sigma}{R})$) in the background of a trap. Since both the position and velocity of A and B are close ($|x_A - x_B| \sim \sigma$), the velocity increase of A & B are almost the same (difference $\sim O(\frac{\sigma^2}{R^2})$). In this manner, the passing of particle C only kicks the center of mass of the A-B pair slightly, leaving the internal motion of the pair unaffected. In another word, the existence of C will not have significant effect on the energy transfer between A and B, but only “dance” with their center of mass. The physics of the “dance” is similar to the dance between two particle. As is shown in fig.9, the particles with energy close to each other tends to form a pair with small internal energy and the pair’s internal energy transfer is relatively stable.

The argument above still holds in many-particle case. Once we start from some configuration where n particles have a set of close energy levels $\{E_n\}$ and another m

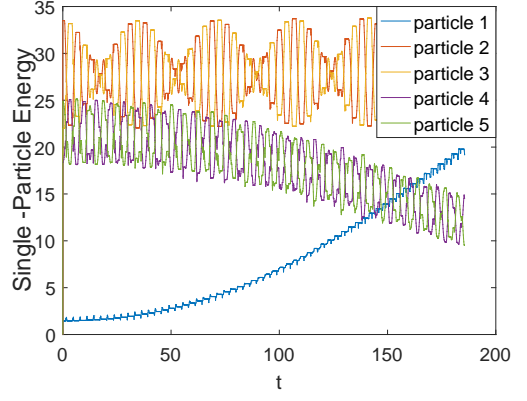


FIG. 9. evolution of single-particle energy

particles have another set of energy levels close to each other $\{E_m\}$, and $\{E_n\}$ is quite different from $\{E_m\}$, we will find these two systems oscillating on the energy level diagram at low frequency. The discussion above gives us some pictures about the non-ergodic state. For these state, life time is rather long so that once the system reach such configuration (or certain energy distribution), it will take a long time (more than 10^4 periods for $N=5$ case) to decay.

B. Thermalization condition

The main obstruct to get an thermalized state (which can be examined by observing distribution) is the low frequency oscillation mentioned before. Because once these modes are excited, the relaxing time could be very long ($>10^4$). As a result, to achieve ergodic state, we have to avoid such low frequency oscillation. According to our discussion before, the solution is to make internal energy of each two-particle pair not “too large”. Though it is impossible to express the internal energy of every pair in terms of the total energy E , we can estimate it by the average energy, which is $\frac{E}{N}$. At least they are of the same order. The thermalization condition could be given by:

$$F_0 \sigma \sim \frac{E}{N} \quad (9)$$

As is shown in fig.10 above, the critical point for reaching “Boltzmann-like” distribution (later we will verify that it is Boltzmann distribution) is $F_0 = 500$ ($F_0 = 1000$ (we always set $\sigma = 1$), while the average energy ~ 1000 , as we expected, they are of the same order. As a supplementary proof of our argument, fig.11 and fig.12 show the great difference of single-particle energy between two examples of below and above the thermalization threshold ($F_0 = 200$ & $F_0 = 1000$ for $N = 10, E = 10000$): in the former one there is always some particle maintained at high excitation, while in the latter the system probably goes to ergodic. To date, we have verified that the

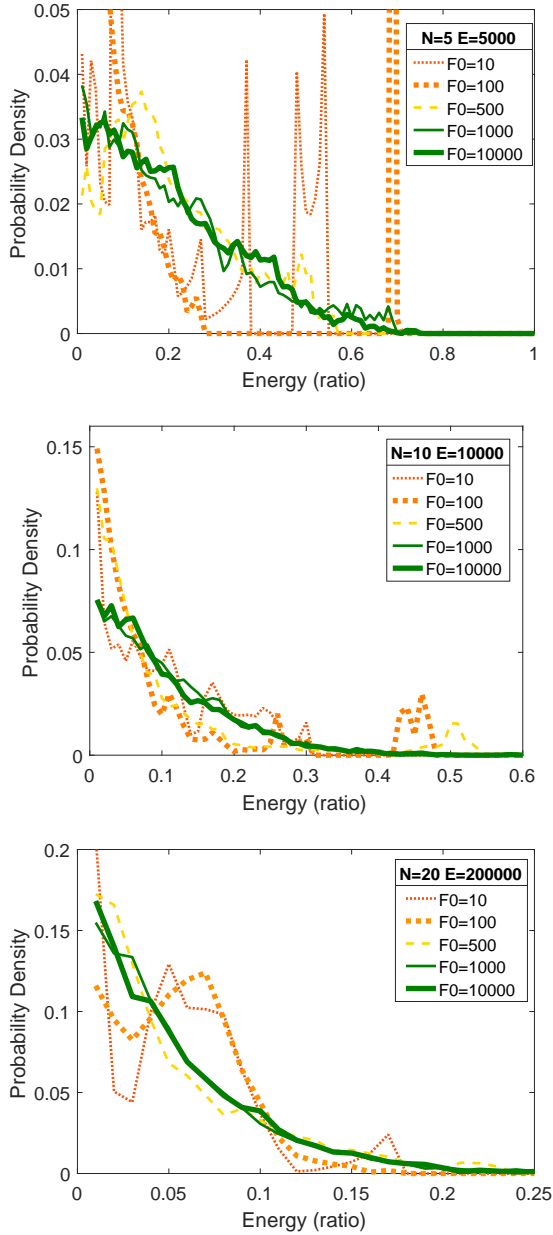


FIG. 10. the energy distribution measured in ~ 10000 time units, as will be verified later, **green** curves corresponds to Boltzmann distribution; **red** curves are obviously non-Boltzmann, while the **yellow** ones are intermediate case, represent “thermalization threshold”. In three figures for different N , we choose E/N identical ($=1000$), and thermalization is reached at $F_0 = 500$ - $F_0 = 1000$, which is consistent with our prediction in Eq.9

threshold of thermalization, which is $\frac{NF_0\sigma}{E} \sim 1$, and corresponding feature of their energy distribution in two side of the threshold.

One may think that this condition only means that the energy transfer in every collision is much smaller than the energy interval. But this is not the whole story. The essential difference between these two regime lies

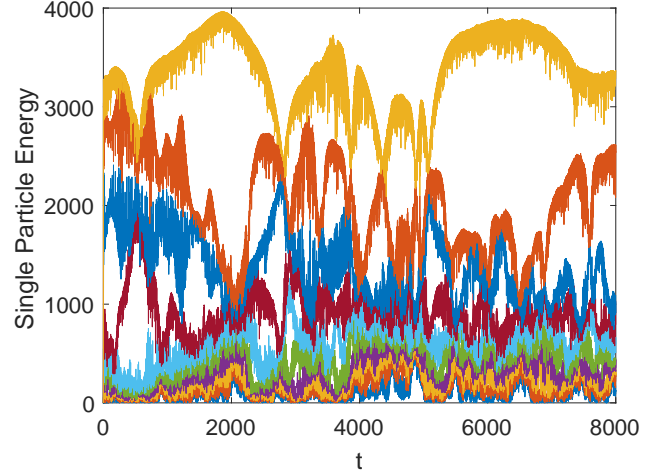


FIG. 11. energy of each particle, $F_0 = 200$

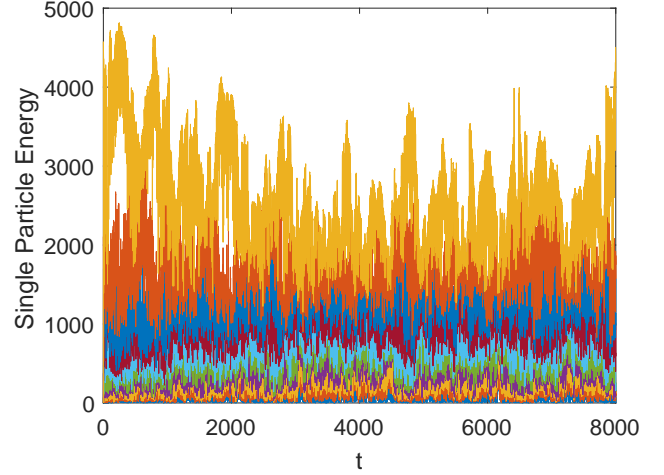


FIG. 12. energy of each particle, $F_0 = 1000$

in whether the energy transfer in every collision is correlated: In thermalizable regime, the energy transfer in every collision is much smaller than the energy interval, which definitely slows down the energy transfer. What is more, because of this, the particles is less interfered by other particles so that two-particle analysis survives. It means that for a particle pair, the energy transferred in this collision is correlated with the one in the next time. In this manner, each particle in the pair will pick up some energy in several collisions, and then return it back to its partner – which is just what the long term beat effect tells us. Thus the particles energy is localized in certain value. On the contrary, if we go to non-thermalizable regime, the energy transfer is so fast that for each particle don’t remember their partners. As a result, the energy transferred in every collision between two particles are no longer correlated, which is equivalent to say that two-particle analysis breaks down. Instead, the energy transfer is completely random, with a non-zero

amplitude. On the single-particle energy diagram, what we expected to see is a “one dimensional random walk”, so energy levels quickly spread around the diagram.

To sum up, the thermalization threshold not only tells us whether the amplitude of energy transfer in every collision is small enough compared to particles’ energy, but also shows whether the “correlation time” of particle pair is much longer than the characteristic time of the system (the oscillation period).

C. Verifying Boltzmann distribution

Thermalization could have different definition. In our system, the “thermalization” we want to find means “losing all the memory of initial state”. One of the most important information of initial state is energy distribution.

For an isothermal system, the energy distribution of the whole system follows the Boltzmann distribution in equilibrium state. However, to our knowledge, there is not any obvious conclusion about the distribution for an isolated system where the total energy is conserved.

But intuitively, one will expect that if we measure the energy of a subsystem, e.g. one particle, then we will get a Boltzmann distribution because the rest part of the system serves as a bath for this particle. The temperature of this isolated system is defined according to $Nk_B T = E$. It is evident that this argument only hold when the energy of the single particle is not too big — if one particle take up 50% of the total energy, the rest could no longer be thought of as a good bath.

In the first picture below, we verify this argument by measuring the energy distribution of every particle at $N=10$ for different F_0 at $E=1000$ (parameters here satisfy thermalizing condition). In the other two, we tested different N .

To take the first one as an example, Y axis is logarithmically scaled. X axis is the ratio between single particle energy (where half of interaction is taken into account) and total energy of the system. The blue dotted line is the predicted Boltzmann distribution (normalized according to counts). Notice that normalizing of the Boltzmann line only change the intercept, leaving slope untouched, which means the slope is the only thing to compare. In Energy ratio smaller than 30%, the experiment (colourful curves) fits well with the prediction. When energy of a single particle is higher, one can think of the “bath” formed by the remaining part has lower temperature, thus counts decrease faster to zero than Boltzmann law.

It is evident from $Nk_B T = E$ that the slope of Boltzmann distribution in this figure only depend on N . That is the reason why we want to measure at different N below.

In fig.13 and fig.14, the curve is slightly deviated from the standard Boltzmann distribution, which is probably due to the contribution of density of states (DOS). Possibility is proportional to Boltzmann exponential factor

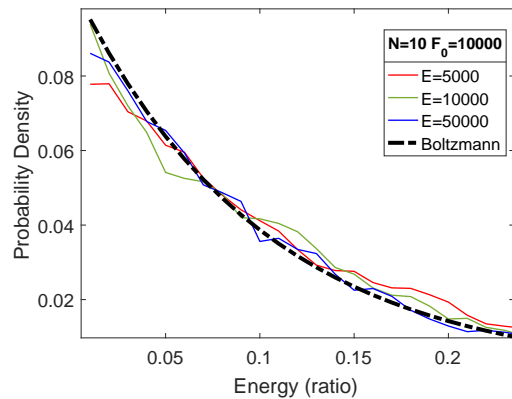


FIG. 13. Energy distribution, $N=10$, $F_0=10000$

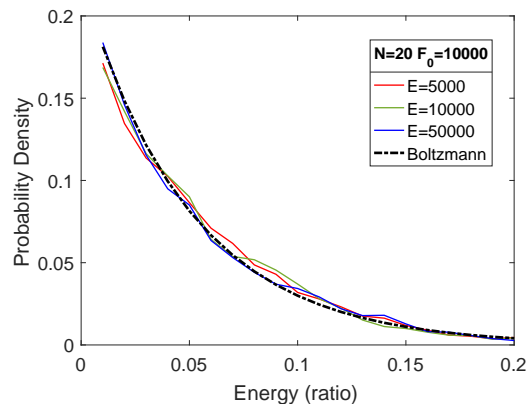


FIG. 14. Energy distribution, $N=20$, $F_0=10000$

multiplied by density of states. The reason why we did not take DOS into account previously lies in that the DOS is a constant for simple harmonic oscillator. However, for simple harmonic oscillators with short range interaction, the energy shell is deformed in the small region of $|x_i - x_j| < \sigma$ so that the DOS is no longer a constant. But since $\sigma \ll R$, one can think of this as a small modification. Therefore, the tendency of the curve in fig.13 and fig.14 is deviated slightly from Boltzmann distribution.

D. Lyapunov Exponents

To see the time scale of “thermalization” and “relaxation” more systematically, we may measure the Lyapunov Exponents. Lyapunov Exponents (LE) describes how fast one orbit diverge from its nearby orbits in phase-space. But for high dimensional system, LE is a spectrum that manifest the instability of the trajectory along each direction. The largest Lyapunov exponents (LLE) reflects the time scale that system lose its memory in phase-space. We will measure the LLEs along our trajectory and plot its distribution.

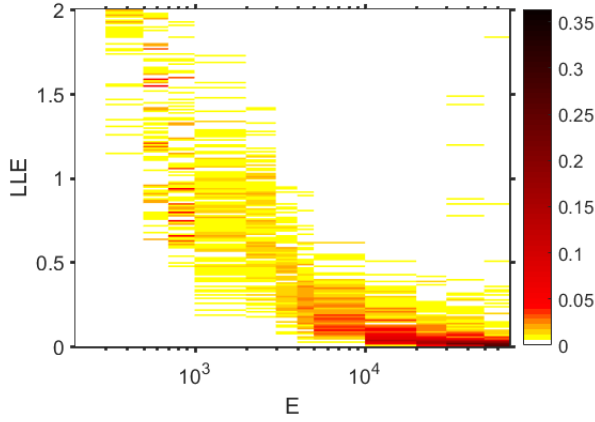


FIG. 15. LLE distribution for $N=5$, $F_0=1000$, scan E. “hot” (reversed)

fig.15 shows the distribution of LLE by color. The LLE decrease with the growth of Energy. The crucial part is near $E=5000$. The most probable value of LLE goes down from 1 to 0.1, which indicate that **the shortest time scale becomes longer than an oscillation period when E is larger than 5000**. And $E=5000$ is exactly our prediction value of thermalization threshold. So there is a correspondence between energy thermalization and LLE. The size of bin (resolution of LLE) in fig.15 is 0.01, so when E goes far beyond the thermalization threshold, the LLE distribution is not that clear. We only know that LLE is concentrated close to zero in high E regime.

E. Shape of Distribution in Phase-space

When describing simple harmonic motion, it is usually convenient to use the language of phase-space (of single particle). In the phase-space, the motion becomes circular, so each of these particles has two independent degree of freedom, i.e., modulus and phase angle. Here, independent means that the simple harmonic oscillation never “mix” these two degrees of freedom. In view of this, when it comes to “thermalization”, one may notice that the thermalization of energy, which is just the modulus, does not ensure the thermalization of phase angle. To distinguish these two kind of meanings of “thermalization”, we will call the process of energy distribution going to equilibrium “thermalization”, while the process of phase angle going to equilibrium “relaxation”. The time scale of thermalization and relaxation could be different in principle. We start with the configuration where particles’ velocities are set to be zero, which means in phase-space the cloud is a rotating narrow ellipse at the beginning. If the time scale of thermalization is much longer than that of relaxation, we will see cloud going to some stable shape in a short time, e.g. a circle in high energy. Meanwhile, the distribution of particle number along radius slowly evolves to Boltzmann distribution.

If the relaxation time is longer than the thermalization time, the cloud will maintain elliptical shape or some oscillation between different shapes for a long time while the radius distribution is already Boltzmann.

To quantify the shape of distribution in phase-space, we defined a shape polarization S :

$$S = \frac{a - b}{a + b} \quad (10)$$

where a and b are long axis and short axis of inertia ellipse in phase space respectively. a, b can be calculated by diagonalizing the inertia tensor I : $I_{xx} = \sum p^2$, $I_{xp} = I_{px} = -\sum xp$, $I_{pp} = \sum x^2$. $S=1$ for line-shape distribution, $S=0$ for circular distribution. The advantage of defining the S lies in that S is independent of all rotating behavior of the cloud in phase-space and thus extract the information of shape alone. One could also use eigenvalues of quadrupole moment Q to define S , since the inertia tensor I is similar to quadrupole moment Q (only different up to a factor and an identity matrix).

The time evolution of S is shown in Fig.16. The top three pannels are the overall value of S , where every data point is the average value of original data over several period (about 2π time unit). The lower six pannels are the original data measured in the beginning and after thousands of time units, which shows the finer structure in one period.

The original data can be decomposed into two components: the background value and the frequent fluctuation (sharp peaks and dips) on the background. The fluctuation is generated from the two-particle transportation process (See Fig.5), e.g. a pair transportation event along the long-axis of the cloud makes a dip. In the thermalized regime (Fig.16), the background value of S is oscillating with an amplitude of 0.2-0.4 and does not decay to zero over 4000 time unit. In the high-energy case, the amplitude of background oscillation is small compared with fluctuation. We assume that over a long enough time, all macroscopic quantity should be constant because the randomness has wash out all possible orders to make entropy as large as possible. Since we see a periodical behaviour of S , we know the whole system doesn’t relax to its equilibrium state.

The oscillating background value of S indicate that the shape of the cloud in phase space is deformed periodically between a circle and an ellipse ($S = 0.4$ means $\frac{a}{b} \sim 2.5$). To further reveal the nature of this oscillating mode, we focus on the low-energy case and plot the distribution of the cloud in the phase space as Fig.17. The time interval between each pannels is $0.1 \cdot 2\pi$ time units. The direction of the yellow arrows and red arrows are the eigenvector of inertia tensor, while their lengths are the square root of correspondent eigenvalue (I take the squareroot to maintain the length unit). In most of the pannels in Fig.17, the long and short axis are rotating and extending or contracting continuously. The exception is the 3rd and 4th pannel in the first row, 2nd and 3rd pannel in the second row, 1st and 2nd pannel in the third row. At those

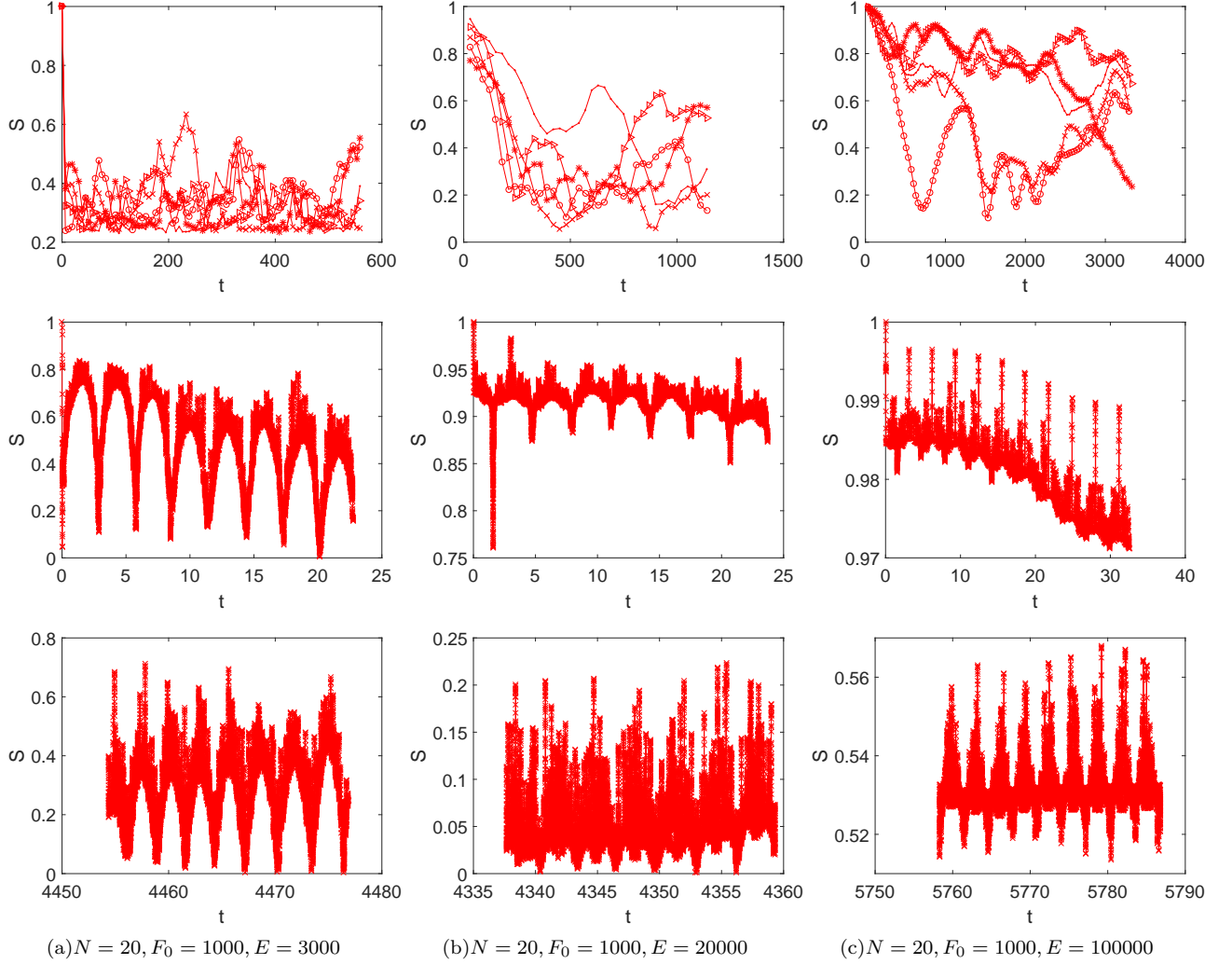


FIG. 16. Time evolution of S in low-energy regime(a), intermediate(b), high-energy regime(c). The overall value (top three pannels), where every point represent the average of original data over several periods, show that S decays to a low value in a short time in low-energy case, but persist for a relative long time in high-energy case. The snapshots of original data at beginning and after thousands of periods evolution are shown in the lower six pannels. The finer structure of $S(t)$ indicates that there is some long-lasting oscillating mode. Especially in low-energy case, the amplitude is more conspicuous.

moment, the long and short axis are almost equal, giving the system a chance to choose a new preferred axis to polarize. The whole picture of this collective mode can be described by Fig.18, which is consistant with the pattern of time evolution of S shown in Fig.19.

To sum up, the existence of the long-lasting oscillation of S indicate that the system does not relax to its equilibrium state in terms of shape although it is already thermalized in terms of energy distribution. With this long-lasting mode, the radius R of the cloud will keep oscillating, enabling the breathing mode to last for a long time.

V. CONCLUSION

We studied the nonequilibrium property of one-dimensional classical gas with finite range repulsive interaction. We first studied the relation between breathing mode frequency and interaction parameter as well as total energy. We found the breathing frequency could be estimated by 6. And the mechanism behind this relation is that the momentum transfer which happens instantly in collision saves the particles some time from traveling this distance. So the physics is completely the same as hardcore particle. We found that the thermalization behavior is controlled by the competition between the interaction strength and the average energy. We point out that there could be two independent time scales in simple

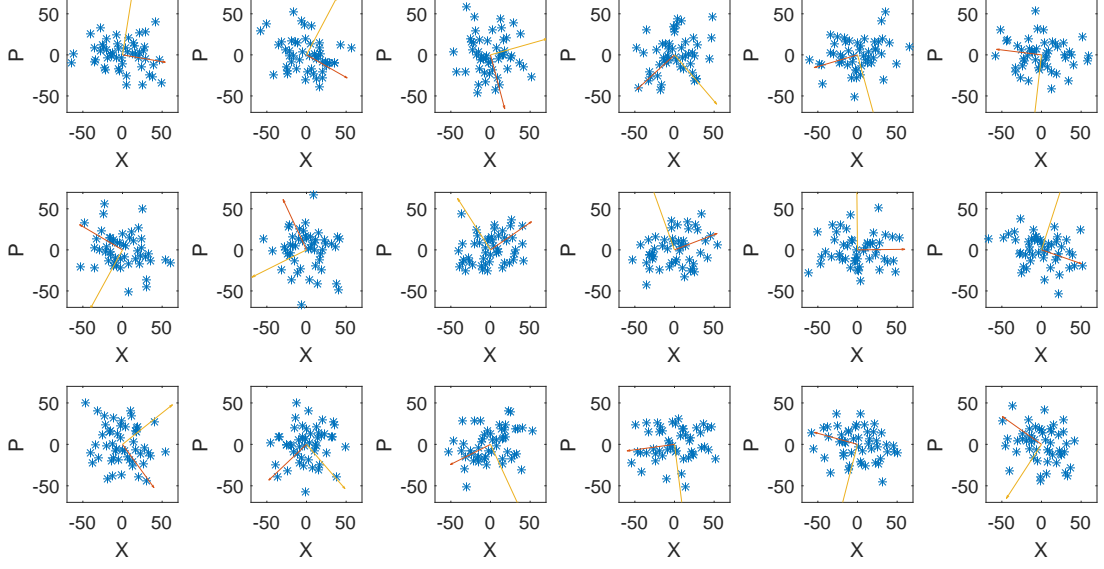


FIG. 17. Distribution in phase-space after evolving for about 500 time units ($N = 50, F_0 = 1000, E = 30000$). Please notice that the yellow(red) arrows shows the length of long(short) axis of inertia ellipse, which is perpendicular to the long(short) axis of distribution cloud. For instance, if the yellow arrow lies in p-axis, it means the long axis of distribution cloud is lying along x-axis.

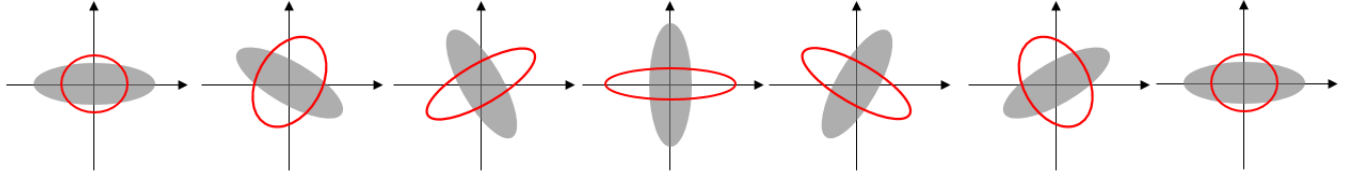


FIG. 18. Schematic description of the excited mode. Red ellipse is the shape of cloud in low-energy regime when there is repulsive interaction. Gray cloud is the imaginary shape of cloud when there is no interaction, they are plotted here as a reference. One may think of the effect of interaction as a kind of potential that prefer to place particles along x axis, because in low energy regime the system is not allowed to be squeezed too much along x axis since doing this cost a large amount of interaction energy.

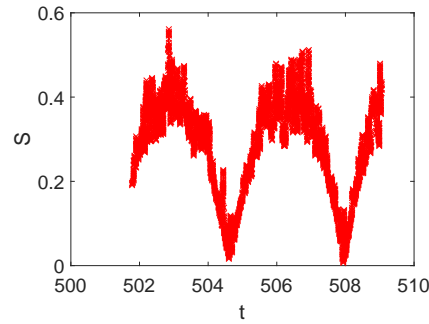


FIG. 19. Time evolution of S after evolving for about 500 time units ($N = 50, F_0 = 1000, E = 30000$). The oscillating behaviour of S persists over 500 time units.

harmonic system in principle. One of them corresponds to the relaxation time of the energy distribution. The other one corresponds to the relaxation time of the angular distribution in phase space, which will determine the decay rate of the amplitude of the breathing mode. We

have shown that in the low-energy regime, although the energy distribution reach Boltzmann distribution within several periods of oscillation, the shape keep oscillating for thousands of periods.

-
- [1] F. Dalfovo, S. Giorgini, M. Guilleumas, L. Pitaevskii, and S. Stringari, Phys. Rev. A **56**, 3840 (1997).
 - [2] D. S. Jin, J. R. Ensher, M. R. Matthews, C. E. Wieman, and E. A. Cornell, Phys. Rev. Lett. **77**, 420 (1996).
 - [3] F. Dalfovo, S. Giorgini, L. P. Pitaevskii, and S. Stringari, Rev. Mod. Phys. **71**, 463 (1999).
 - [4] S. Stringari, Phys. Rev. Lett. **77**, 2360 (1996).
 - [5] E. Haller, M. Gustavsson, M. J. Mark, J. G. Danzl, R. Hart, G. Pupillo, and H.-C. Ngerl, Science **325**, 1224 (2009).
 - [6] F. Jin, T. Neuhaus, K. Michielsen, S. Miyashita, M. A. Novotny, M. I. Katsnelson, and H. D. Raedt, New Journal of Physics **15**, 033009 (2013).
 - [7] W. Tschischik, R. Moessner, and M. Haque, Phys. Rev. A **88**, 063636 (2013).
 - [8] W. Tschischik and M. Haque, Phys. Rev. A **91**, 053607 (2015).
 - [9] D. Guéry-Odelin, F. Zambelli, J. Dalibard, and S. Stringari, Phys. Rev. A **60**, 4851 (1999).
 - [10] K. R. Yawn and B. N. Miller, Phys. Rev. E **56**, 2429 (1997).
 - [11] A. A. El-Zant, Phys. Rev. E **58**, 4152 (1998).
 - [12] T. Tsuchiya and N. Gouda, Phys. Rev. E **61**, 948 (2000).